NATIONAL AERONAUTICS AND SPACE ADMINISTRATION

Technical Memorandum 33-782

Heterogeneous Reaction of Ozone With Aluminum Oxide

JET PROPULSION LABORATORY
CALIFORNIA INSTITUTE OF TECHNOLOGY
PASADENA, CALIFORNIA

August 15, 1976

NATIONAL AERONAUTICS AND SPACE ADMINISTRATION

Technical Memorandum 33-782

Heterogeneous Reaction of Ozone With Aluminum Oxide

L. F. Keyser

JET PROPULSION LABORATORY
CALIFORNIA INSTITUTE OF TECHNOLOGY
PASADENA, CALIFORNIA

August 15, 1976

CONTENTS

TABLES

CONTENTS (Contd)

ABSTRACT

Rates and collision efficiencies for ozone decomposition on aluminum oxide surfaces were determined. Samples were characterized by BET surface area, X-ray diffraction, particle size, and chemical analysis. Collision efficiencies were found to be 2×10^{-9} to 2×10^{-10}. This is many orders of magnitude below the value of 10^{-6} to 10^{-5} needed for appreciable long-term ozone loss in the stratosphere. An activation energy of 7.2 kcal $mole^{-1}$ was found for the heterogeneous reaction between $-40^{\circ}C$ and $+40^{\circ}C$. Effects of pore diffusion, outgassing and treatment of the aluminum oxide with several chemical species were also investigated.

1.0 INTRODUCTION

The Space Shuttle will introduce submicron aluminum oxide particles into the stratosphere. Because of low settling rates for these finely divided particles, residence times in the stratosphere are estimated to be several years. Since aluminum oxide catalyzes ozone decomposition by means of a heterogeneous surface reaction, the stratospheric ozone concentration could conceivably be reduced by a significant amount if the surface reaction is sufficiently fast.

Previously, Schwab and Hartmann[1] studied the decomposition of ozone on several metal oxides, including aluminum oxide. Using a flow method, they determined an activation energy for the heterogenous reaction between 20°C and 150°C. More recently, Ellis and Tometz[2] used a flow method to study ozone decomposition on aluminum oxide and other materials at room temperature. Atiaksheva and Emelianova[3] also studied the decomposition, using a flow method at temperatures between 30°C and 90°C. While the present study was in progress, a similar investigation was begun by Fujiwara[a], using both flow and static methods at temperatures between 25°C and 200°C.

The principal objective of the present study was to determine the rate and the collision efficiency of the heterogeneous reaction between ozone and aluminum oxide. Since it is difficult to duplicate stratospheric conditions in exact detail in the laboratory, it is important to determine the extent to which various parameters (such as pressure, temperature, diffusion, surface condition, etc.) may affect the measured rate. Once the magnitudes of these effects are known, it is possible to extrapolate the laboratory rate to the

---

[a]T. Fujiwara, Ames Research Center, NASA, Moffett Field, CA 94035

stratosphere with some confidence and to put limits on the possible errors involved. The following is a report of surface rate measurements and the effects of various parameters on these rates.

2.0 EXPERIMENTAL

Both static and flow methods were used to study the reaction of ozone with aluminum oxide. The static system is shown schematically in Fig. 1. It consists of a quartz reaction cell of known volume near 90 cm^3, constant temperature circulator, and a photometer. A known weight of aluminum oxide was added to the quartz cell and outgassed under vacuum at room temperature for one hour or more before the addition of ozone. For most experiments, a new sample of aluminum oxide was used for each run. Ozone concentrations were followed photometrically, using 253.7 nm light. Decay rates of ozone were displayed on a strip chart recorder. Temperatures between 230 and 310°K were controlled by means of a constant temperature circulator.

The flow system used for several measurements of ozone decomposition is shown in Fig. 2. It consists of an ozone generator, needle valve, flow meter, vertical flow tube, stagnation region to trap the aluminum oxide particles, and an optical cell.

Commercial, laboratory-prepared and solid rocket motor exhaust samples of aluminum oxide were used in the studies. They were characterized by X-ray diffraction, BET surface area, particle size, and chemical analysis. Long-path infrared absorption was used to determine the products of outgassing.

Matheson UHP grade oxygen and electronic purity hydrochloric acid were used without further purification. Ozone was prepared as needed by a high frequency discharge in oxygen. Gamma alumina was prepared by the procedure outlined in reference (1).

3.0 RESULTS

3.1 Characterization of Samples

Sample analysis is needed to relate the observed rate constants to properties, such as surface area, crystal structure, porosity, etc. Complete sample analysis is also important when making comparisons with results obtained in other laboratories. The aluminum oxide samples were characterized by X-ray diffraction, BET surface area, particle size, chemical analysis, and outgassing studies.

Aluminum oxide exhibits many crystalline forms[4], some of which are shown schematically in Fig. 3. The transition forms occur during the thermal decomposition of the tri-hydroxides. However, some of the transition aluminas can also be produced by other methods. These metastable forms of alumina are of interest, since they generally are highly reactive and have large specific surface areas.

X-ray diffraction determines the crystalline forms of aluminum oxide which are present. The semi-quantitative results are summarized in columns 3 and 4 of Table 1. It is interesting to note that the rocket exhaust samples consist mainly of the high-temperature forms (theta and alpha), with only minor amounts of the gamma form. X-ray analysis does not reveal which form is present on the surface, but it is very unlikely that the low-temperature gamma phase could be present in large concentration on the surface of the high-temperature phases.

Surface areas were measured, using nitrogen adsorption. Analysis of the results using the BET method gave values for the specific surface areas shown in column 5 of Table 1.

Particle size was measured, using optical microscopy for sample A, since this sample of gamma alumina was used most extensively in the studies. The average radius quoted for Sample B is the manufacturer's value. Particle size is shown in the last column of Table 1.

Chemical analysis and outgassing studies are summarized in Table 2. The results show that recoverable HCl and H_2O are adsorbed on the rocket exhaust samples.

3.2 Rate Constants - Static System

Surface reaction rates were determined by following the decay of ozone in the presence of a known amount of aluminum oxide. Typical results are shown in Fig. 4. Plots of the logarithm of ozone concentration (optical density) versus time are nonlinear. This indicates that the reaction is not first order in gas-phase ozone concentration. However, it is possible to define an experimental rate constant in terms of the initial slope of the semi-log plot as follows:

$$k = [Al_2O_3]^{-1} (-d \ln[O_3]/dt) \qquad (1)$$

where $[Al_2O_3]$ is the concentration of aluminum oxide in grams cm^{-3}.

In general, the rate constant was calculated from the slope after a one to two minute delay. This allowed the system to stabilize following the addition of ozone and oxygen. The initial rate is the maximum observed rate and represents a worst case for ozone destruction. Ozone decay rates are corrected for the decomposition of ozone in the absence of aluminum oxide; in most cases, the correction is considerably less than 5%. Rate constants obtained in this way are shown in Table 3. Except for the flow system results discussed below, all the rate constants reported here were measured using the static system.

3.3 Collision Efficiency

A collision efficiency for ozone decomposition may be defined by equating the loss rate of ozone to the collision rate on the aluminum oxide surface

$$\frac{-d \ln[O_3]}{dt} = k[Al_2O_3] = \frac{1}{4} \gamma \bar{v} \Sigma [Al_2O_3]$$

$$\gamma = \frac{4k}{\bar{v}\Sigma} \qquad (2)$$

where γ is the collision efficiency, k is the observed rate constant, $\bar{v}$ is the ozone molecular velocity, Σ is the specific surface area of the aluminum oxide sample and $[Al_2O_3]$ is in units of grams cm^{-3}. Collision efficiencies obtained from the observed ozone decay rates and the BET surface areas are shown in column 4 of Table 3. They are in the range 2×10^{-10} to 2×10^{-9}, which is many orders of magnitude lower than the figure of 10^{-6} to 10^{-5}, which is needed for appreciable ozone destruction in the stratosphere. No significant correlation exists between surface areas and the collision efficiencies; this is important evidence that diffusion effects are small and will be discussed more fully below.

3.4 Rate Constants - Flow System

As the aluminum oxide particles slowly settle through the stratosphere, they are exposed on all sides to ozone. However, in the rate constant measurements previously described in the static system, the particles are not suspended but are located at the bottom of the quartz cell containing the ozone. To determine whether suspending the aluminum oxide has an effect on the observed ozone destruction rate, measurements were also carried out in the flow system shown in Fig. 2. In this case, a stream of ozone in oxygen was passed through

a vertical flow tube and then through an optical cell in which the ozone concentration was determined. Ozone decay rates were then calculated from the flow rate and the decrease in ozone concentration when aluminum oxide is added to the flow tube. The rate constant for ozone decay in the flow system is defined as

$$k = \frac{F}{V - V_c} \frac{1}{[Al_2O_3]} \ln \frac{[O_3]_o}{[O_3]} \qquad (3)$$

where F is the flow rate in $cm^3\ sec^{-1}$, V is the volume of the vertical flow-tube reactor, and V_c is the volume of the aluminum oxide sample. Results of the flow studies are shown in Table 4. They agree reasonably well with those obtained using the static system and with results of other independent flow-system studies.

3.5 Diffusion

High surface area solids generally are extremely porous. Most of the measured BET surface area is located within the pore structure, and the exterior surface represents only a small fraction of the total. Depending on the relative rates of diffusion and surface reaction, diffusion into the pore structure can affect the measured rate constants. This can be seen by considering two extreme cases. First, if diffusion is rapid compared to the surface reaction, ozone can diffuse into all parts of the pore structure before reaction occurs. In this case, the entire surface of the aluminum oxide is exposed to ozone and the observed reaction rate is the true surface reaction rate. If the rate of diffusion is slow compared to the rate of surface reaction, ozone will react before it diffuses very deeply into the pore structure and only a small fraction of the surface is exposed to ozone. In this case,

the observed rate is very much smaller than the true surface reaction rate. It is important to determine the true surface reaction rate in order to extrapolate the laboratory results to the stratosphere, since the particle size distribution occurring there could be considerably different from that of the laboratory samples.

The effect of diffusion can be expressed in terms of a factor, ϵ, as follows

$$k_{expt'l} = \epsilon\, k_{surface} \tag{4}$$

where $0 \leq \epsilon \leq 1$. ϵ is the fraction of surface available for reaction. When diffusion is rapid compared to the rate of surface reaction, $\epsilon = 1$ and the observed rate is the true surface reaction rate. Several methods can be used to estimate the minimum value of ϵ and thus test for the effects of diffusion. These methods will be discussed below.

Under conditions where the mean free paths of the gas molecules are small compared to the average pore radius, the rate of diffusion depends inversely on the pressure. If diffusion effects are important, ϵ will depend on pressure, and the observed rate should increase as the pressure is lowered. Figure 5 shows the results of varying the pressure on a high surface area alumina. The observed rate increases by about a factor of three at the lower pressures. For the low surface area SRM samples (Fig. 6), the observed rate constant is independent of pressure. These results indicate that the minimum value of ϵ is about 0.3. This applies only to pores with radii greater than about 0.1 μm. For smaller pores, the mean free path becomes large compared to pore size and other methods must be used to estimate diffusion effects.

Another test for diffusion effects uses the collision efficiency. When diffusion is rapid compared to the surface reaction rate, the entire BET surface area is available for reaction, and the observed reaction rate will be proportional to the surface area. Another way of stating the same thing is that under rapid diffusion conditions, the rate per unit BET area should be independent of the area. The rate per unit area is just the collision efficiency. Columns 3 and 4 of Table 3 show that the collision efficiency is independent of surface area within a factor of 10. This indicates that ϵ is greater than about 0.1.

A more exact method of treating diffusion uses a model for the pore structure to calculate ϵ[5-7]. For spherical particles

$$\epsilon = \frac{3}{h}\left[\frac{1}{\tanh h} - \frac{1}{h}\right], \tag{5}$$

where $h = R(k_s/V_g D)^{1/2}$. R is the particle radius, k_s is the true surface reaction rate in $cm^3 g^{-1} sec^{-1}$, V_g is the specific pore volume in $cm^3 g^{-1}$ and D is the diffusion coefficient which is given by the relation

$$D = \frac{2}{3}\bar{v}\bar{r}. \tag{6}$$

$\bar{r}$ is the average pore radius. To obtain a value for ϵ, it is convenient to define a quantity Φ.

$$\Phi \equiv R^2 k_e / V_g D = \epsilon h^2, \tag{7}$$

where k_e is the experimentally observed rate constant. All of the quantities in Φ can be measured or estimated.

There is a correlation between specific surface area and average pore radius[8,9]. The minimum value for $\bar{r}$ expected for the high surface area aluminas is 1 nm. As a worst case calculation, this value is used to estimate the diffusion coefficient from equation (6).

In calculating ε, it is convenient to first obtain ε as a function of h from equation (5). Using these results, values of $\Phi \equiv \varepsilon h^2$ can then be obtained. A plot of ε vs Φ enables one to read ε for various experimental values of Φ. The plot of ε vs Φ used in these calculations is shown in Fig. 7.

For sample A, the laboratory prepared γ-alumina, the calculation was carried out for particle radii between 0.1 and 1000μm and specific pore volumes between 0.01 and 0.5 cm^3g^{-1}. The results are shown in Fig. 8. Values reported for pore volume measurements of aluminum oxide samples are generally in the range 0.07 to 0.4 cm^3g^{-1}[10,11]. Taking the worst case as V_g = 0.05 cm^3g^{-1} and R = 100 μm, ε = 0.6. Diffusion effects are expected to be less than a factor of two for the sample of γ-alumina.

Results of these tests for diffusion effects are summarized in Table 5 and show that the maximum effect based on collision efficiencies could be a factor of 10. However, the estimate obtained from the spherical particle model should be more reliable and shows that the effect is less than a factor of 2.

3.6 Effect of HCl and H_2O Vapor

Since HCl and H_2O vapor are present in the SRM exhaust, it is important to determine whether treating the aluminum oxide samples with these gases affects the observed rate constants. The results of these studies are summarized in Table 6. HCl activates the aluminum oxide for ozone destruction.

Water vapor deactivates the samples. The largest effect was observed, using the activated alumina; the effects are reduced in the CRM samples which had previously been exposed to HCl and H_2O vapor in the exhaust gases.

3.7 Effect of Sample Size

To determine whether sample size has any effect on the observed ozone decay, weights were varied for the activated alumina sample. The results (shown in Table 7), indicate no significant variation in observed rates for a ten-fold change in sample weight.

3.8 Temperature Variation

Rates of ozone decomposition on γ-aluminum oxide were determined for temperatures in the range +40°C to -40°C. Since stratospheric temperatures are in the range -60°C at 15 km to -5°C at 40 km, the experimental conditions approximate temperatures in the stratosphere. The results indicate that the rate decreases at lower temperature. At -40°C the rate is lower than the room temperature rate by a factor of 30. The results may be plotted in Arrhenius form:

$$\ln k = \ln A - E_{act}/RT \ , \qquad (8)$$

in order to determine an activation energy for the reaction. The plot of ln k vs. 1/T is shown in Fig. 9. The line drawn through the points is a least-squares fit of the data, and its slope gives an activation energy of 7.2 ± 1.5 kcal mole^{-1}. This is in reasonably good agreement with previous measurements at temperatures below 100°C. Schwab and Hartmann[1] report 6.4 kcal mole^{-1} for temperatures between 20°C and 100°C. Atiaksheva and

Emelianova[3] report 9.1 kcal mole^{-1} between 30°C and 90°C. Fujiwara[a] obtained 6.1 kcal mole^{-1} between 25°C and 90°C; however, at temperatures between 140°C and 200°C, the activation energy is reported to be 23.8 kcal mole^{-1}. Although Fujiwara corrected for the homogeneous ozone decomposition, these corrections became very large above 100°C. The apparent increase in activation energy at higher temperatures may be due to failure to fully correct for the homogenous decomposition. The combined results of this and other studies indicate that at stratospheric temperatures, rates of ozone decomposition should be at least an order of magnitude lower than that observed at room temperature.

3.9 High-Temperature Outgassing

The aluminum oxide exhaust particles are exposed to elevated temperatures immediately before deposition in the stratosphere. Temperatures are approximately 3000°C in the rocket combustion chamber and 400°C to 500°C in the plume at 30 exit diameters. To determine whether exposure of aluminum oxide to elevated temperatures has an effect on the ozone decomposition rate, samples were calcined under vacuum at temperatures up to 700°C.

Weighed samples of aluminum oxide were placed in a quartz optical cell housed in a tube furnace. Following calcination, the cell was allowed to cool to room temperature. Without exposing the samples to the atmosphere, ozone and oxygen were added to the cell. Photometry at 253.7 nm was used to follow the decay rate of ozone. The results are summarized in Table 8.

For Sample A (γ-alumina), the rate of ozone decay increases by a factor of 230, following calcination at 300°C for 3 hours. Calcining at 700°C for

---

[a]T. Fujiwara, Ames Research Center, NASA, Moffett Field, CA 94035

3 hours causes no further significant increase in the ozone decomposition rate. Exposure to 6.7 kPa (50 torr) of oxygen has little effect, but exposure to the laboratory atmosphere for 17 hours deactivates the sample below the initial ozone loss rate. Pressure and temperature during calcination of the sample are shown in Fig. 10. These curves show that most of the outgassing occurs below 400°C. This observation, plus the fact that heating to 700°C has a similiar effect as heating to 300°C, indicates that no further increase in the ozone decomposition rate will occur at the even higher temperatures that occur in the rocket exhaust. Results for Sample SRMC are similar to those obtained for Sample A, except that the sample is deactivated more rapidly when exposed to oxygen or to the laboratory atmosphere.

Effects of diffusion on the ozone decay rates observed following calcination were investigated, using the pore structure model described above. The results indicate that for Sample A the correction could be as large as a factor of 30. That is, the true surface reaction rate could be as high as 9×10^4 cm^3 g^{-1} sec^{-1} ($\gamma = 7 \times 10^{-6}$). For SRMC, γ could be as high as 2×10^{-6}. However, exposure to the atmosphere deactivates the calcined samples in 24 hours or less. Thus, the effective lifetime in the stratosphere as highly reactive centers for ozone destruction is limited. This point will be discussed again below in estimating ozone decomposition rates in the stratosphere.

3.10 Prolonged Exposure to Ozone

To determine whether repeated exposure of aluminum oxide to ozone can activate the sample for ozone decay, two series of experiments were carried out. In the first, ozone and 6.7 kPa (50 torr) of oxygen were repeatedly added to the same sample of aluminum oxide in the static system. During each run, ozone was in contact with the sample for 10 minutes, the amount

of aluminum oxide having been adjusted so that the half-life of ozone was approximately 5 minutes. Between additions, the cell was evacuated for 15 minutes. The results are shown in Fig. 11, where the relative rate of ozone decay is plotted vs. accumulated contact time with Sample A (γ alumina).

In another set of experiments, ozone was continuously produced by photolysis of oxygen in the cell containing the aluminum oxide sample. Oxygen pressures were 40 kPa (300 torr) and 80 kPa (600 torr). The cell was evacuated for 10 minutes before determining the ozone decay rate. The results, also given in Fig. 11, show an initial increase, followed by a decrease in the relative rate for long-term exposure to ozone.

The present results show that repeated exposure to ozone for one to two hours activates the aluminum oxide for ozone decomposition, but continued exposure for 20 to 24 hours has a slightly deactivating effect. Deactivation was also observed by Fujiwara[a] in both flow and static experiments below 1.3 kPa (10 torr) and by Ellis and Tometz[2] in a flow system. However, Schwab and Hartmann[1] report a ten-fold increase in activity after 6 hours, which then remains level when γ-alumina is exposed to ozone in a flow system. The combined results of this and other studies show that prolonged exposure to ozone can activate aluminum oxide, but the magnitude of the effect is less than a factor of 10.

3.11 Estimate of Ozone Loss in the Stratosphere

Results obtained in this study may be used to estimate the effect of aluminum oxide on stratospheric ozone concentrations. The rate of ozone decomposition in the stratosphere may be written

---

[a]T. Fujiwara, Ames Research Center, NASA, Moffett Field, CA 94035.

$$-d \ln[O_3]/dt = k\,[Al_2O_3] \qquad (9)$$

To obtain the O_3 destruction rate, concentrations of aluminum oxide in the stratosphere must be estimated. This will be done below for two cases.

a. In exhaust plume during one shuttle flight

Current calculations of injectants per flight give a value of about 9 metric tons of aluminum oxide into a 3 km band at 30 km. Taking a plume radius of 1 km, this results in an aluminum oxide concentration of 9.55×10^{-10} g cm^{-3}. Using this value along with a rate constant of 60 cm^3 g^{-1} sec^{-1} results in an ozone half-life of 0.38 year. This is close to the half-life of 0.5 year estimated for the reaction of ozone with oxygen atoms.

b. Long-term loss in the stratosphere due to repeated flights

Steady-state aluminum oxide concentrations in the stratosphere may be estimated from

$$[Al_2O_3]_{stratosphere} = FWT/V \ , \qquad (10)$$

where F is the number of shuttle flights per year (F ~ 50), W is the weight of aluminum oxide released per flight (W ~ 9×10^6 g in a 3 km band at 30 km), T is the residence time (T ~ 2 years), and V is the volume of a hemispherical shell at 30 km (V = 7.74×10^{23} cm^3). The resulting aluminum oxide concentration is 1.16×10^{-15} g cm^{-3}.

The surface reaction rate required to equal ozone loss by reaction with oxygen atoms in the stratosphere may be obtained from equation (9) by using the steady-state aluminum oxide concentration. Taking 0.5 year as the approximate half-life of ozone with respect to the oxygen atom reaction results in k = 4×10^7 cm^3 g^{-1} sec^{-1} or $\gamma = 3 \times 10^{-3}$ for Sample A. In order that

ozone loss on aluminum oxide be small compared to natural losses, γ should be 10^{-6} or lower. Collision efficiencies observed in this study are all in the range 10^{-9} to 10^{-10}, except for an estimated maximum value of 10^{-6} to 10^{-5} following high-temperature outgassing.

The high collision efficiencies observed following outgassing above 300°C are rapidly reduced when the samples are exposed to air. Thus, if the exhaust particles deposited in the stratosphere have collision efficiencies as high as 10^{-5}, their lifetime as highly reactive particles is limited to a few days. Equation (10) may be used to estimate the effective concentration of these reactive particles by taking the lifetime T ~ 0.01 year. This results in an activated aluminum oxide concentration of 5.8×10^{-18} g cm^{-3}. Using a value of 9×10^{4} cm^{3} g^{-1} sec^{-1} for the surface reaction rate results in an ozone half-life of 4.2×10^{4} years. Although the above calculations can be considered only approximate, they do show that the long-term ozone decay rate in the stratosphere due to aluminum oxide is many orders of magnitude slower than the natural loss rate.

3.12 Oxygen Atom Recombination

Since atomic oxygen and ozone are rapidly interconverted in the stratosphere, it is possible that recombination of oxygen atoms on aluminum oxide could affect the ozone concentration. Collision efficiencies for atomic oxygen recombination have been measured on various surfaces. The results vary widely, depending on the experimental conditions. For pyrex in a flow system at 130 Pa (one torr), values of 10^{-4} to 10^{-5} were reported[12,13]; however, at pressures below 1.3 mPa (10^{-5} torr) in an atomic beam mass spectrometer, collision efficiencies on pyrex as high as 0.3 to 0.5 have been found[14,15]. For aluminum oxide, a value of 2.1×10^{-3} was obtained in a flow system at 6.7 Pa (5×10^{-2} torr)[16].

Reactions of atomic oxygen in a pure oxygen atmosphere are as follows

$$O + O + M \xrightarrow{k_1} O_2 + M$$

$$O + O_2 + M \xrightarrow{k_2} O_3 + M$$

$$O + O_3 \xrightarrow{k_3} 2O_2$$

$$O + Al_2O_3 \xrightarrow{k_s} \frac{1}{2} O_2 + Al_2O_3 \ .$$

In the stratosphere, reaction (1) is slow, compared to the other reactions, and will not be considered further. In Table 9, the loss of atomic oxygen by reactions (2) and (3) is compared to the estimated surface loss at various altitudes. Rate constants and concentrations used are those given by Nicolet[17]. The surface reaction rate was calculated, using a specific surface area of 200 $m^2\ g^{-1}$ and $[Al_2O_3] = 1.2 \times 10^{-15}\ g\ cm^{-3}$.

As seen in Table 9, the surface recombination rate is orders of magnitude slower than loss by reaction (2) at all altitudes considered. Compared to reaction (3), the surface reaction is not important (less than 0.1%) for $\gamma \leq 10^{-1}$ up to 40 km, the maximum altitude for aluminum oxide injection by the Space Shuttle. If the measured value of 2×10^{-3} for the collision efficiency is correct, surface recombination should have a negligible effect on the ozone concentration. This rough calculation is in agreement with recent model calculations of Cadle, Crutzen and Ehhalt[18]. These authors report no significant difference in the ozone loss with and without surface recombination of oxygen atoms for $\gamma = 10^{-3}$ to 10^{-4}.

Because of the wide variations that can occur in measured collision efficiencies, additional studies of atomic oxygen recombination on aluminum oxide should be made to determine whether $\gamma \leq 10^{-1}$ on these surfaces.

4.0 SUMMARY

a. Ozone decay rates and collision efficiencies were determined using various aluminum oxide samples having a range of crystal structures and surface areas.

b. Collision efficiencies are in the range 2×10^{-10} to 2×10^{-9}.

c. Rate of ozone decomposition on aluminum oxide surfaces decreases as the temperature is lowered.

d. Activation energy for the heterogeneous reaction is 7.2 kcal $mole^{-1}$.

e. Suspending aluminum oxide particles in a flow has no large effect on the observed rates.

f. Pressure variation and calculation show that pore diffusion has no large effect on the observed reaction rates. The maximum possible effect is a factor of 10.

g. HCl activates aluminum oxide for O_3 destruction.

h. H_2O deactivates aluminum oxide for O_3 destruction.

i. After outgassing at 300°C to 700°C, ozone decomposition rates are increased 230 to 300 times. Exposure to air for less than 24 hours deactivates the samples.

j. Worst-case estimates show that the ozone destruction rate in the exhaust plume could be comparable to the ozone loss rate by reaction with oxygen atoms.

k. Estimates indicate that long-term ozone loss in the stratosphere is negligible.

l. Loss of ozone by oxygen atom recombination on aluminum oxide is negligible if γ for the recombination is less than 10^{-1}.

Table 1. Characterization of Aluminum Oxide Samples

		X-RAY ANALYSIS[a]			
	SAMPLE	FORM	CRYSTALLITE SIZE	SPECIFIC SURFACE AREA	PARTICLE SIZE
A	Laboratory Preparation	Gamma	50A	123 m^2 $gram^{-1}$	$\bar{r} \leq 50\mu m$
B	Degussa Aluminum Oxide-C	Gamma	65	116	$\bar{r} = 0.02$
C	Alcoa F-1 Activated Alumina	Boehmite, major; Gamma, minor	50	208	-
D	Baker Reagent Powder	Alpha, major; Theta, trace	-	9.1	-
SRM-A[b]	JPL Rocket Motor Inside Tank	Alpha, major; Gamma, delta, minor	-	4.8	-
SRM-B	JPL Open Burn Inside Tank	Theta, major; Gamma, delta, Alpha, minor	-	5.4	-
SRM-C[b]	JPL Rocket Motor Inside Tank	Alpha, major; Gamma, delta, minor	-	1.8	-

[a] Analyses carried out by Technology of Materials, Santa Barbara, CA.

[b] Gaseous residence time in rocket was approximately 15 msec for SRM-A, approximately 90 msec for SRM-C. SRM-C more closely approaches conditions expected for space shuttle solid booster rockets.

Table 2. Chemical Analysis and Products of Outgassing

SAMPLE	Wt. % Cl	WEIGHT LOSS 180°C, 2 HRS	IR OF PRODUCTS
SRM - A	3.47	-4.8%	HCl, H_2O
SRM - B	0.74	-1.7%	-
Activated Alumina	0.01	-	-

Table 3. Ozone Decay Rates and Collision Efficiencies, Static System, T = 298°K, $P(O_2)$ = 80 k Pa (600 torr)

SAMPLE	k(cm^3 $gram^{-1}$ sec^{-1})	SPECIFIC SURFACE; AREA (m^2 $gram^{-1}$)	COLLISION EFFICIENCY
A	9.5[a]	123	7.8×10^{-10}
B	1.81	116	1.6×10^{-10}
C	23.2	208	1.1×10^{-9}
D	0.25	9.1	2.8×10^{-10}
SRM-A	0.191	4.8	4.0×10^{-10}
SRM-B	0.102	5.4	1.9×10^{-10}
SRM-C	0.30	1.8	1.7×10^{-9}
Activated Charcoal	12.0	-	-
ZnS	0.31	-	-
MnO_2	0.113	-	-

[a] $P(O_2)$ = 6.7 k Pa (50 torr).

Table 4. Comparison of Flow and Static Results

SAMPLE	FLOW RATE ℓmin^{-1}	k_3 (FLOW) $cm^3 g^{-1} sec^{-1}$	k_3 (STATIC) $cm^3 g^{-1} sec^{-1}$	REFERENCE
Activated Alumina	1.0 - 1.5	4.7	8.9 - 23.2	This work
SRM-B	0.6 - 0.8	0.29	0.102	This work
Pelletized Al_2O_3 Powder	28.3	8.55	-	Ellis and Tometz
Activated Alumina	0.1 - 0.3	2.7	-	Atiaksheva and Emelianova

Table 5. Summary of Diffusion Tests

METHOD	POROUS STRUCTURE	RESULTS
Pressure Variation	$r \geq 0.1$ μm	$\epsilon \geq 0.3$
Collision Efficiency vs. Surface Area	All sizes	$\epsilon \geq 0.1$
Spherical Particle Model	$r \leq 0.1$ μm	$\epsilon \geq 0.5$

Table 6. Effect of HCl and H_2O

SAMPLE	k ($cm^3\ g^{-1}\ sec^{-1}$)	HCl[a]	H_2O[b]
SRM-A	0.191	-	-3.7%
SRM-B	0.102	+18%	-26%
Activated Alumina	23.2	+100%	-74%

Samples outgassed at 298°K for one hour

P_T = 80 kPa (600 torr) O_2; P (ozone) = 270 Pa (2 torr)

[a] HCl = 40 kPa (300 torr) for 2 hours

[b] H_2O = 3.3 kPa (25 torr) for 30 minutes

Table 7. Effect of Alumina Sample Weight on k

Weight, mg	k
2.2	19.8 $cm^3\ g^{-1}\ sec^{-1}$
4.1	27.1
11.6	31.3
11.7	29.2
20.9	26.6
AVERAGE	26.8

Samples outgassed at 298°K for one hour, P_T = 80 kPa (600 torr) O_2, P_{O_3} = 80 Pa (0.6 torr)

Table 8. Effect of Outgassing[a]

SAMPLE	INITIAL RATE	AFTER 3 HRS AT 300°C	AFTER 3 HRS AT 700°C	6.7 kPa (50 TORR) O_2 FOR 30 MIN	97 kPa (730 TORR) AIR FOR 1 HR	97 kPa (730 TORR) AIR FOR 17 HRS
A (γ-alumina)	12.3	2.81×10^3	2.92×10^3	2.16×10^3	1.11×10^2	3.77
SRM-C	1.06	3.25×10^2	3.98×10^2	34.8	7.22	2.36

[a]Rate constants ($cm^3\ g^{-1}\ sec^{-1}$) measured at 24°C.

Table 9. Loss of Atomic Oxygen

ALTITUDE	$k_2\ [O_2]\ [M]$	$k_3\ [O_3]$	$k_S\ [Al_2O_3]/\gamma$
20 km	$7.9 \times 10^2\ sec^{-1}$	$2.9 \times 10^{-3}\ sec^{-1}$	$3.5 \times 10^{-5}\ sec^{-1}$
30	31	2.6×10^{-3}	3.5×10^{-5}
40	1.2	1.3×10^{-3}	3.7×10^{-5}
50	6.9×10^{-2}	2.7×10^{-4}	3.9×10^{-5}

REFERENCES

(1) G.M. Schwab and G. Hartmann, Z. Physik. Chem. 6, 56 (1956).

(2) W.D. Ellis and P.V. Tometz, Atmos. Environ. 6, 707 (1972).

(3) L.F. Atiaksheva and G.I. Emelianova, Zh. Fizich. Khim. 47, 2113 (1973).

(4) K. Wefers and G.M. Bell, Technical Paper No. 19, Alcoa Research Laboratories (1972).

(5) A. Clark, "The Theory of Adsorption and Catalysis," Academic Press (1970).

(6) A. Wheeler, "Catalysis," Vol. 2, Part 2, pp. 105-165, Reinhold Corp. (1955).

(7) A. Wheeler, "Advances in Catalysis," Vol. 3, pp. 250-326, Academic Press (1950).

(8) J. Sanlaville, Genie Chem. 78, 1C2 (1957).

(9) J.H. deBoer, Angew. Chem. 70, 383 (1958).

(10) L.C. Drake and H.L. Ritter, Ind. Eng. Chen. Anal. Ed. 17, 787 (1945).

(11) D.B. Lippens et. al., J. Catalysis 3, 32 (1964).

(12) F. Kaufman, Prog. Reaction Kin. 1 1 (1961).

(13) J. W. Linnett and D.G.H. Marsden, Proc. Roy. Soc. A234, 489, 504 (1956).

(14) J.A. Riley and C.F. Giese, J. Chem. Phys. 53, 146 (1970).

(15) G.S. Hollister, R.T. Brackman, and W.L. Fite, Planetary Space Sci. 3, 162 (1961).

(16) J. C. Greaves and J.W. Linnett, Trans. Faraday Soc. 55, 1346 (1959).

(17) M. Nicolet, Aeronomica Acta - A, No. 156 (1975).

(18) R.D. Cadle, P. Crutzen and D. Ehhalt, J. Geophys. Res. 80, 3381 (1975).

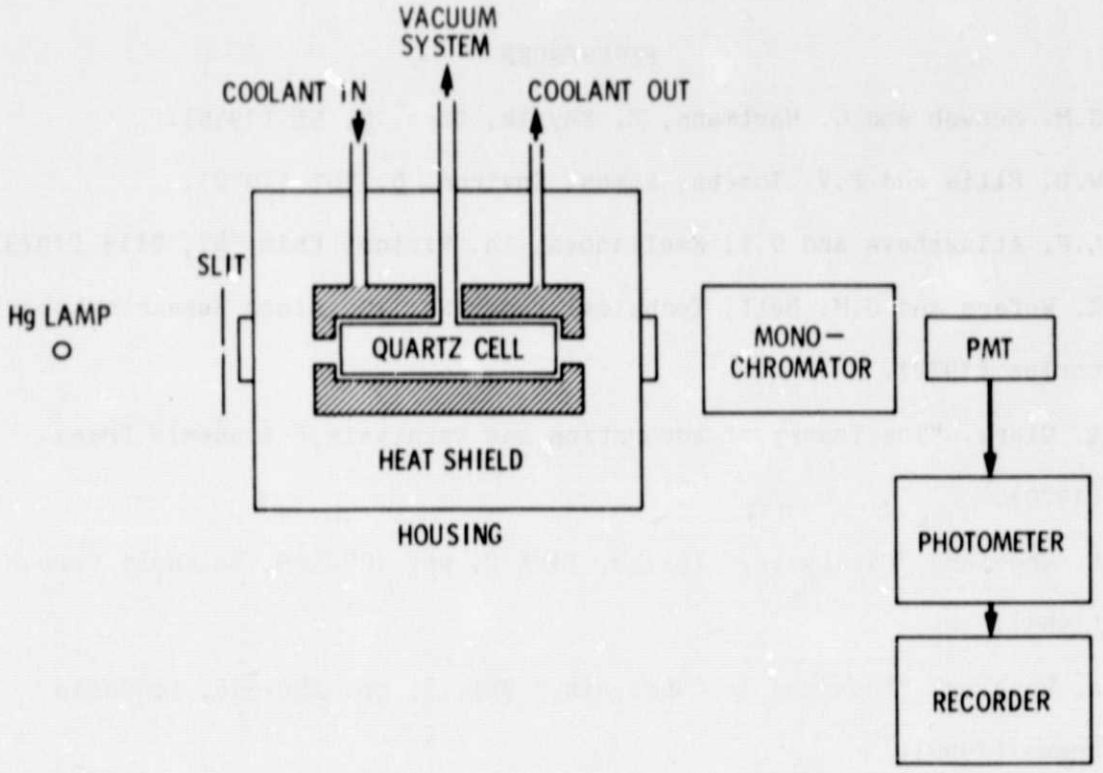

Fig. 1. Schematic of static system

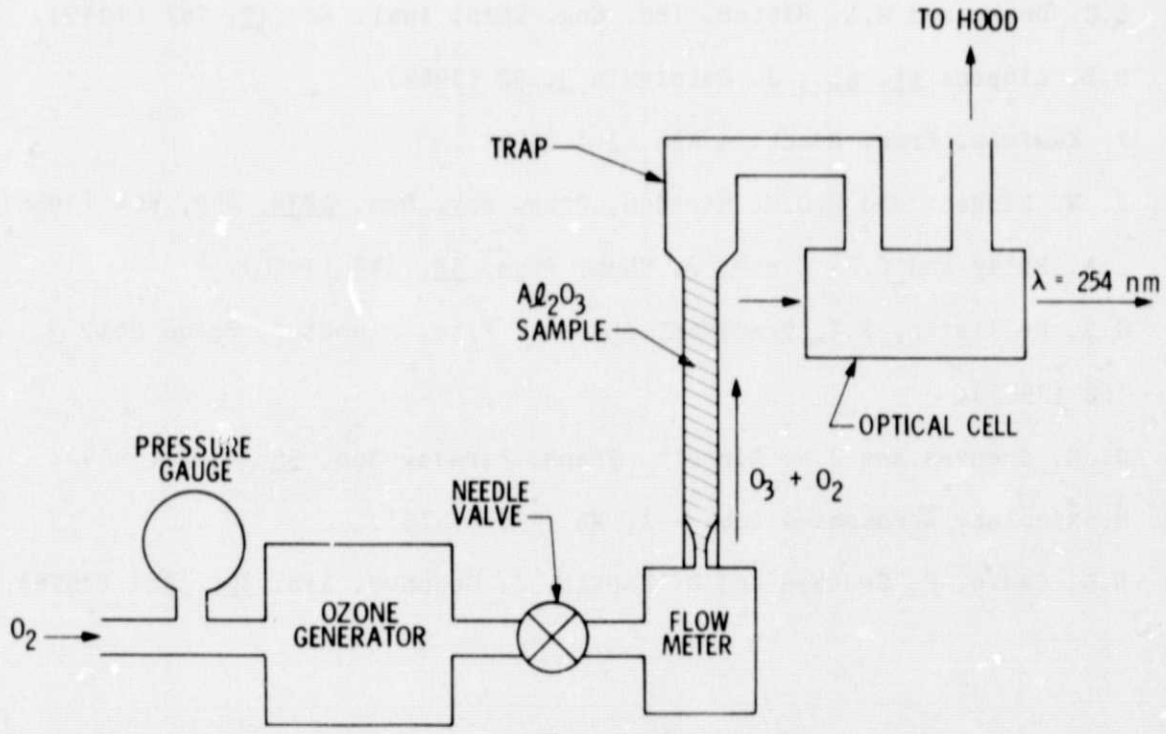

Fig. 2. Schematic of flow system

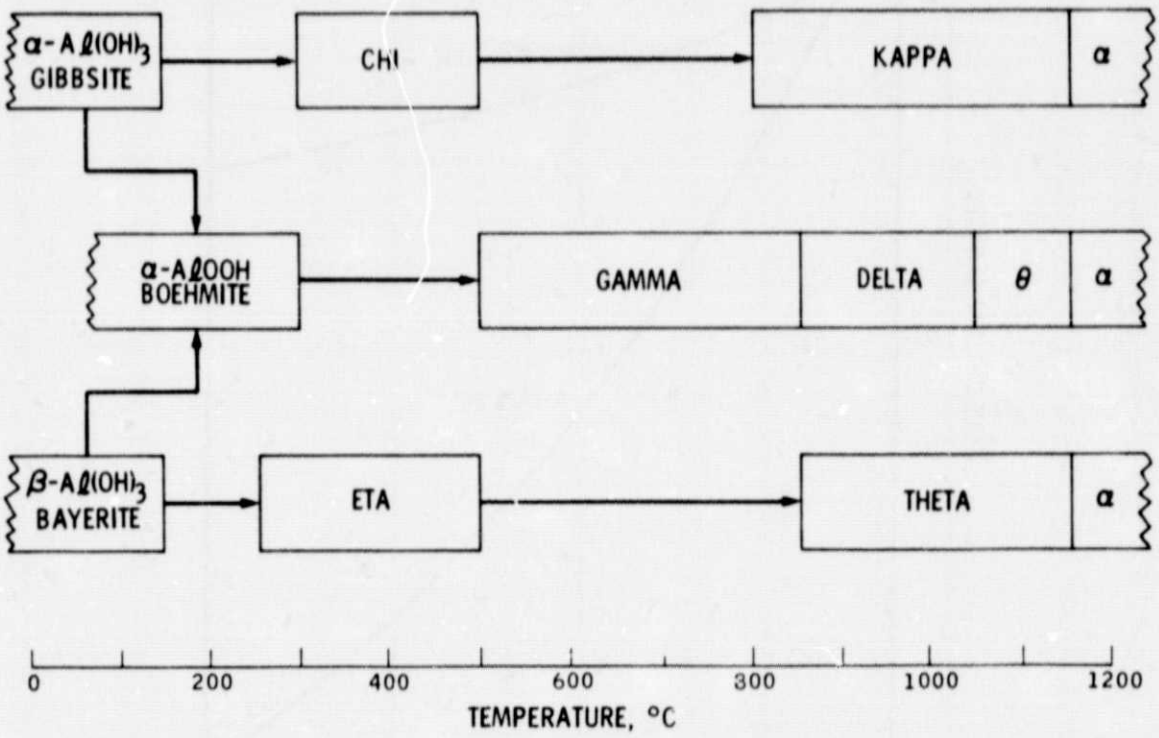

Fig. 3. Transition forms of aluminum oxide

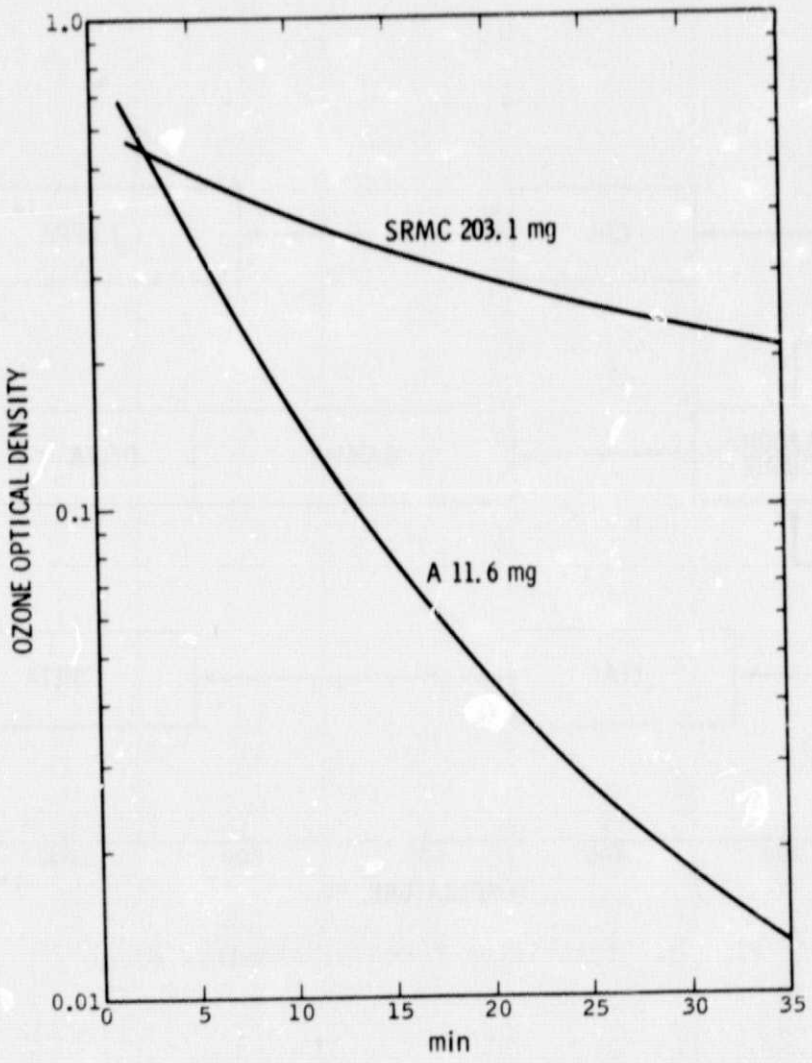

Fig. 4. Plot of ozone optical density vs. time

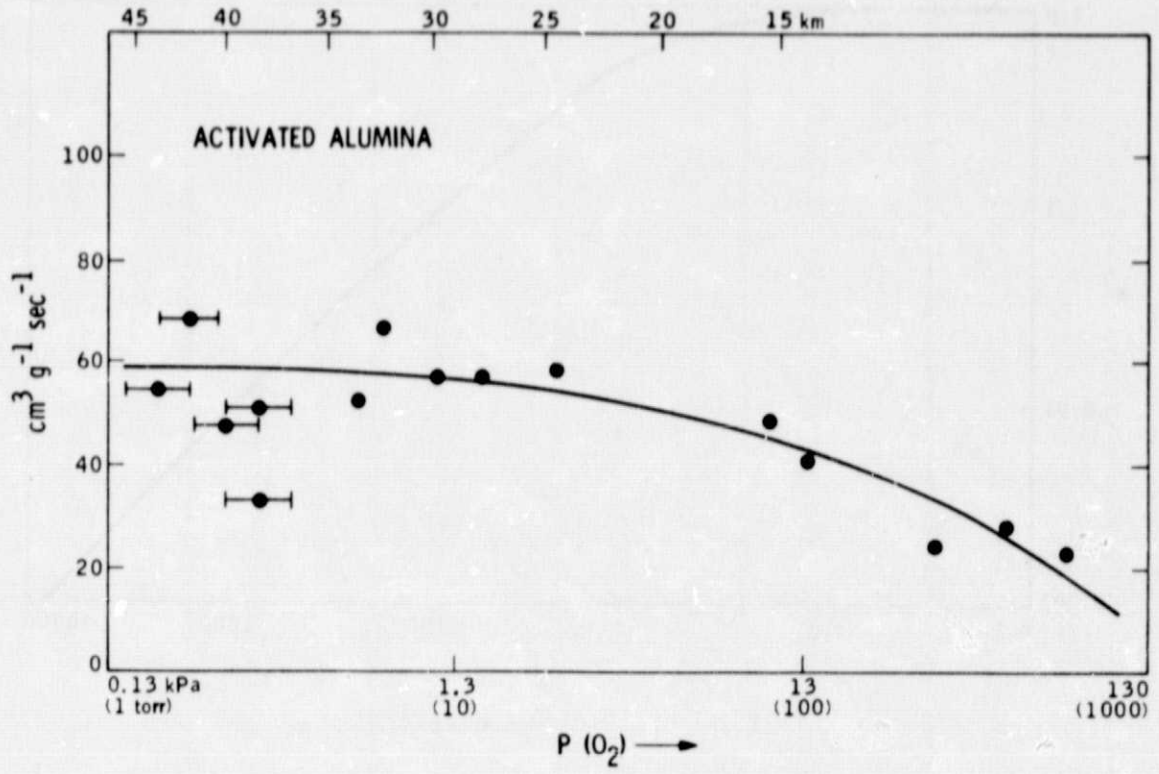

Fig. 5. Observed ozone decay rate vs. oxygen pressure, Sample C - activated alumina

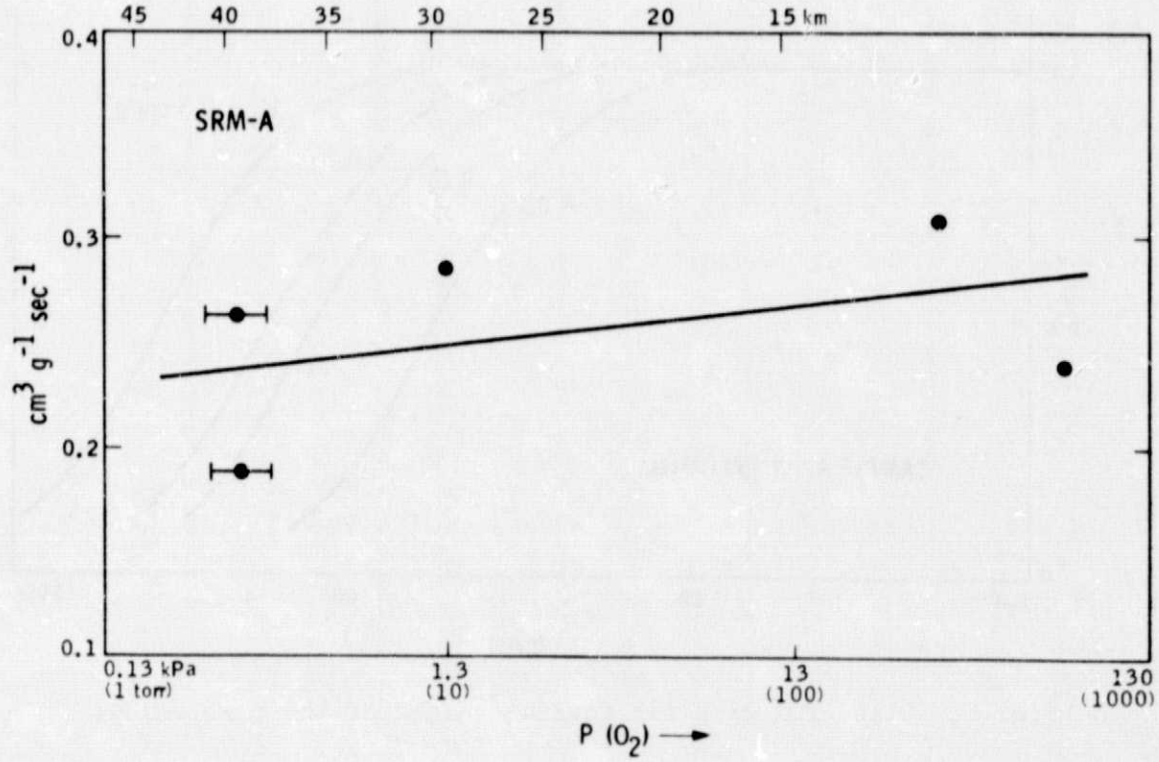

Fig. 6. Observed ozone decay rate vs. oxygen pressure, Sample SRM-A

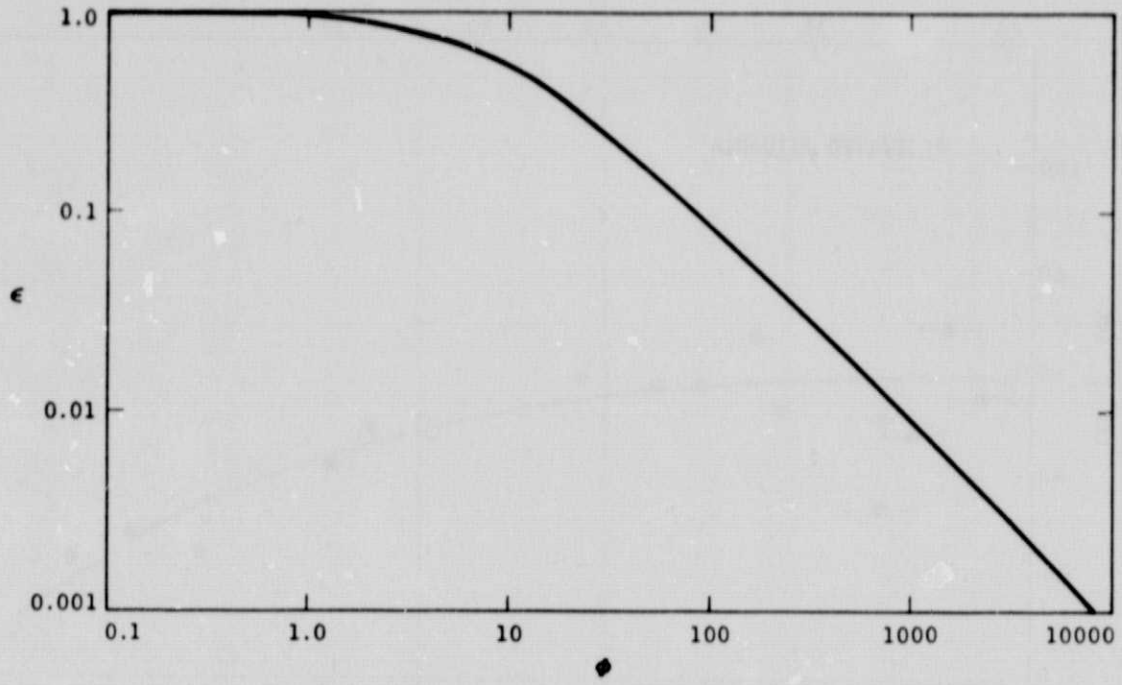

Fig. 7. Plot of ε vs Φ

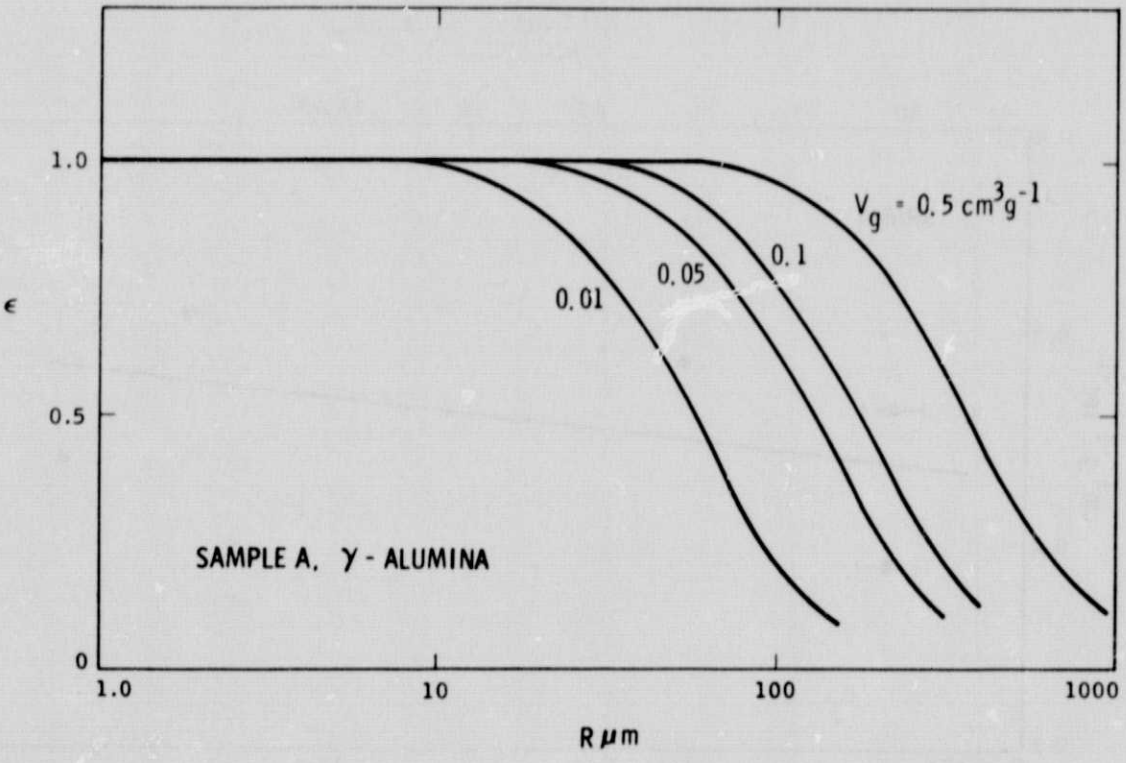

Fig. 8. Plot of ε vs R for several values of the pore volume

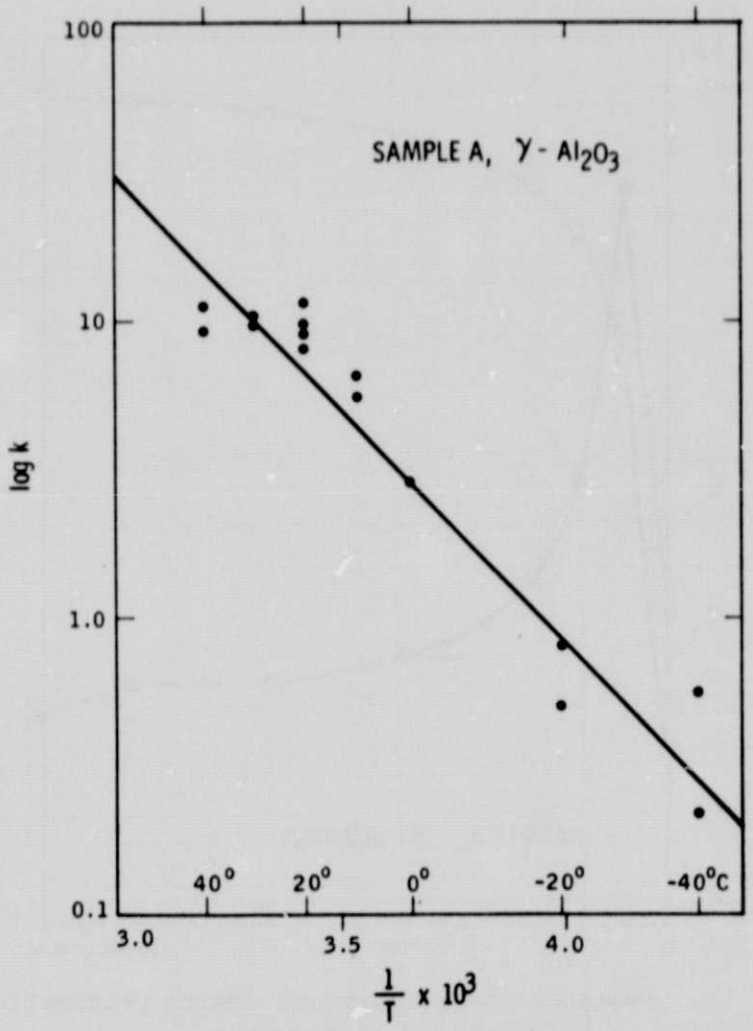

Fig. 9. Arrhenius plot of ozone decomposition rate on Sample A (γ-alumina)

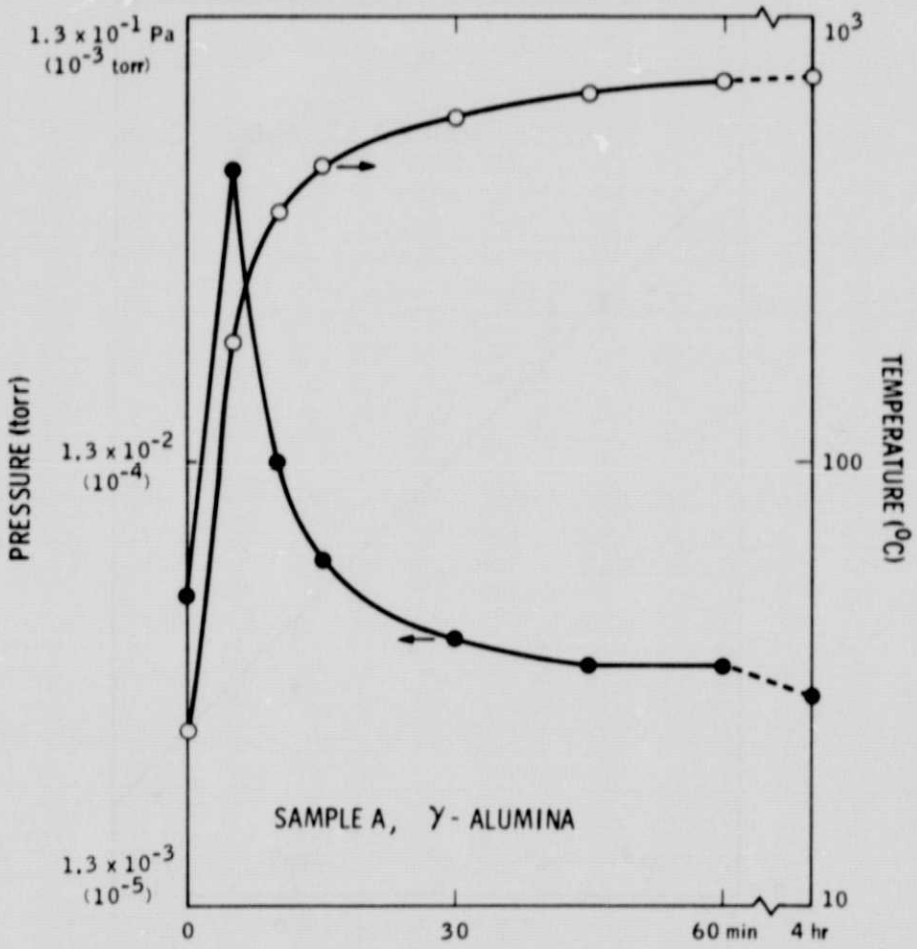

Fig. 10. Pressure and temperature during calcination of Sample A (γ-alumina)

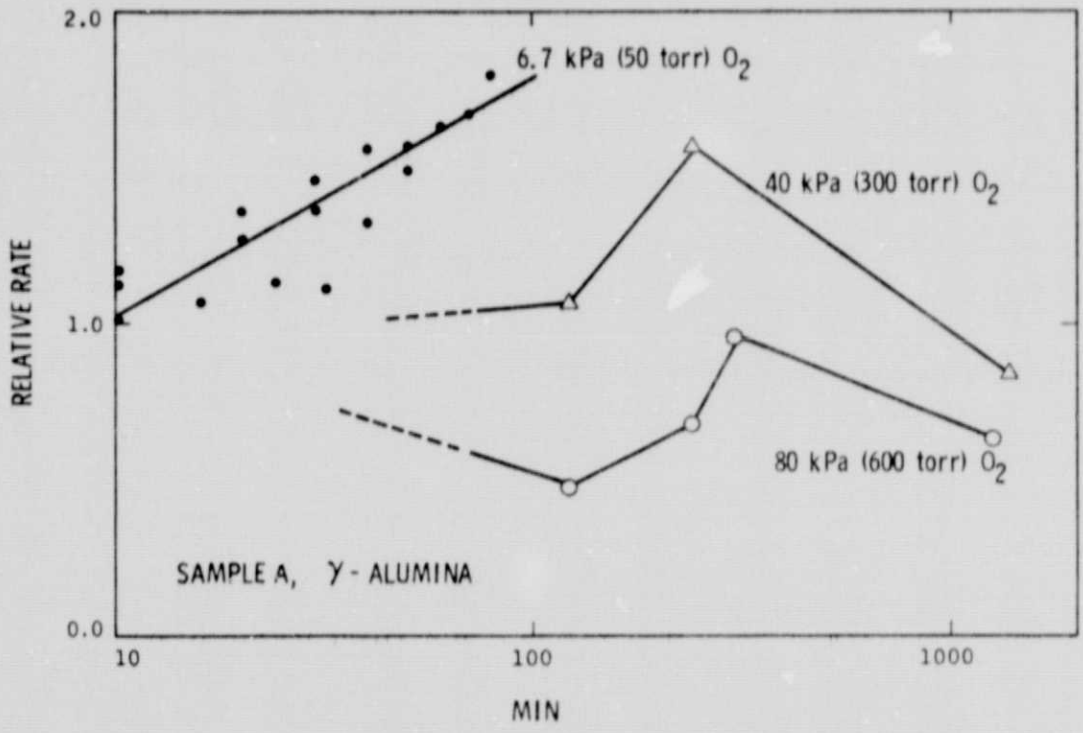

Fig. 11. Relative rate vs. total contact time with ozone